A Guide for Accurate and Repeatable Measurement of the R TH,JC of SiC Packages

Jack Knoll, Christina Dimarino, Cyril Buttay

A Guide for Accurate and Repeatable Measurement of the $R_{TH,JC}$ of SiC Packages

Jack Knoll
Center for Power Electronics Systems (CPES), Virginia Tech
Blacksburg, VA, USA
knolljs@vt.edu

Christina DiMarino
Center for Power Electronics Systems (CPES), Virginia Tech
Blacksburg, VA, USA
dimaricm@vt.edu

Cyril Buttay
Univ Lyon, CNRS, INSA Lyon, Ecole Centrale de Lyon, Université Claude Bernard Lyon1, Ampère, UMR 5005
69621 Villeurbanne, France
cyril.buttay@insa-lyon.fr

***Abstract*—This work aims to understand the influence of various test conditions on the measurement of the junction-to-case thermal resistance ($R_{TH,JC}$) of SiC packages, and identify a procedure that will result in accurate and repeatable measurements. In this study, the $R_{TH,JC}$ measurements of a PCB-embedded half-bridge package containing silicon carbide (SiC) MOSFETs under different test conditions are evaluated. The $R_{TH,JC}$ is determined using the transient dual interface method (TDIM), as reported in the JEDEC JESD51-14 standard. The thermal conductivity of the thermal grease was found to have an impact on repeatability of $R_{TH,JC}$ measurements. $R_{TH,JC}$ measurement sets resulting from alternative copper standoff thickness, negative gate bias, thermal grease thickness, and clamp tip style were found to have statistically significant differences in $R_{TH,JC}$ measurement mean compared to the control set. A method for reducing deviation in $R_{TH,JC}$ measurements is proposed. The $R_{TH,JC}$ of a TO-247 package containing the same SiC MOSFET die is reported to act as a commercially available reference for the PCB-embedded package.**

Keywords—Thermal Resistance, SiC MOSFET, Packaging, Transient Dual Interface Method

I. Introduction

The junction-to-case thermal resistance ($R_{TH,JC}$) is a measure of the thermal performance of a package; lower $R_{TH,JC}$ is preferred to achieve higher heat dissipation. More specifically, $R_{TH,JC}$ is a measure of the junction temperature (T_J) minus the case temperature (T_C) divided by the power dissipated by the device (P) as seen in equation (1). However, $R_{TH,JC}$ is a difficult parameter to measure accurately and repeatably. Concerns about the accuracy of $R_{TH,JC}$ measurement and its use as a figure of merit have been raised repeatedly and as early as 1988 [1]–[3].

$$R_{TH,JC} = \frac{T_J - T_C}{P} \quad (1)$$

Much work has been done to improve $R_{TH,JC}$ and the methods used to measure $R_{TH,JC}$. The impacts of package, material, interconnection, and die size selection on $R_{TH,JC}$ have been explored [4]. Temperature sensitive electrical parameters (TSEP) have been identified to accurately measure the T_J of silicon, silicon carbide (SiC), and gallium nitride [5]–[8]. Methods to measure the $R_{TH,JC}$ of dual-sided packages have even been developed [9].

Some standards call for measuring the T_C using a thermocouple (TC) [10]; however, the location of the case TC can have a significant impact on the measured T_C and, in turn, introduce a high percent error in the measured $R_{TH,JC}$ [11]. The JEDEC JESD51-14 standard on the transient dual interface method (TDIM) was established to eliminate the need for the case TC [12]. The JEDEC JESD51-14 standard has been proven to improve the measurement of $R_{TH,JC}$ [13].

The TDIM states that if two heating curves are measured with two different thermal interface materials (TIMs) placed between the case of the package and the cooler, then the thermal impedance where the two curves diverge should be equal to the $R_{TH,JC}$. The two main factors that impact the accuracy and repeatability of the $R_{TH,JC}$ measurements found using the TDIM are the degree of overlap between the two heating curves before they diverge and the clarity of the divergence point, as seen in Fig. 1a and Fig. 1b, respectively. Both factors depend heavily on the test conditions used to measure the heating curves.

The JEDEC JESD51-14 standard provides some suggested test conditions and procedures and emphasizes the importance of reporting these conditions and procedures along with any results. However, the suggested test conditions and procedures can limit the repeatability and, in some cases, limit the feasibility of measuring the $R_{TH,JC}$. Some test conditions, such as pressure [14], temperature [15], cold plate quality [13], and thermal grease thermal conductivity [13], have been studied to identify their impact on measured $R_{TH,JC}$. The TDIM has also been successfully applied to measure the $R_{TH,JC}$ of SiC packages [16]. However, a thorough analysis of the impact of TDIM test conditions on the measured $R_{TH,JC}$ of SiC packages is missing from the literature. In this work, test conditions are varied to identify their impact on the accuracy and repeatability of the measured $R_{TH,JC}$ of SiC packages.

II. Test Setup and Procedure

In this study, the $R_{TH,JC}$ is measured using the Analysis Tech Phase 12B Thermal Analyzer (Fig. 2) and the JEDEC JESD51-14 standard [12]. First, the temperature dependence of the SiC MOSFET body diode forward voltage was characterized using the calibration oven. The resultant calibration curve had a slope of -442.7 ºC/V and a y-intercept of 1171 ºC. Then, the $R_{TH,JC}$ of

The authors acknowledge the financial support provided by the U.S. Department of Energy Advanced Manufacturing Office through the Wide Bandgap Generation (WBGen) Fellowship at the Center for Power Electronics Systems (CPES) at Virginia Tech (http://www.eng.vt.edu/WBGen).

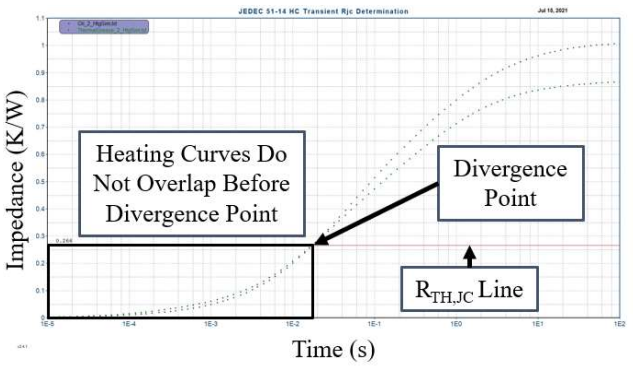

(a)

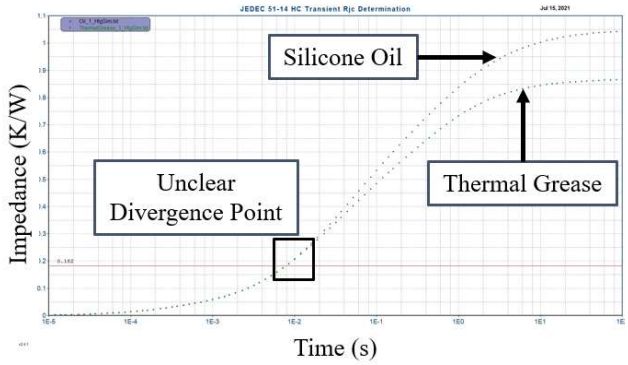

(b)

Fig. 1. Examples of heating curves (a) that do not fully overlap before they diverge and (b) that have an unclear divergence point.

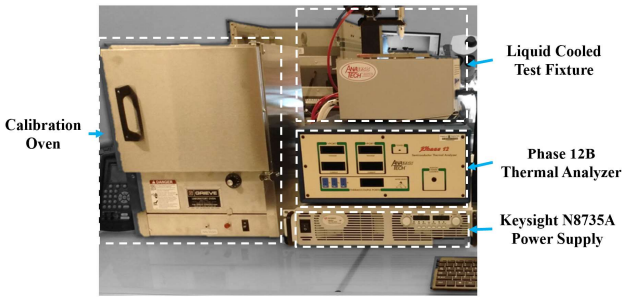

Fig. 2. The Phase 12B Thermal Analyzer from Analysis Tech and its associated calibration oven, liquid cooled test fixture, and external power supply.

a PCB-embedded half-bridge prototype (reported in [17]) that contains those 1.2 kV, 20 mΩ SiC MOSFETs [18] is measured. Prior to these measurements, the $R_{TH,JC}$ for this prototype was unknown.

The PCB-embedded package comes with a unique set of challenges for $R_{TH,JC}$ measurement using the TDIM. It has electrical contacts for the gate, drain, and source of both devices on both sides of the PCB. The copper standoff (shown in Fig. 3a) ensures that only the relevant heat sink area is cooled and that the gate, drain, and source of the device are not electrically shorted. An indium TIM with a thermal conductivity of 0.86 W/(cm°C) is placed between the copper standoff and the cooler to reduce the contact resistance between the two. In following the TDIM, the first and second heating curves are measured with a high thermal conductivity TIM (one of the two thermal greases seen in Table I) and a low thermal conductivity TIM (silicone oil with a thermal conductivity of 0.1 W/mK) applied to the case (as seen in Fig. 3a), respectively. Silicone oil and the two thermal greases were selected because they have different enough thermal conductivities to allow for an $R_{TH,JC}$ measurement to be performed, while also maintaining the same heat flow path in the case. A custom alignment jig is used to secure the copper standoff and the device under test of the PCB-embedded half-bridge package squarely beneath the pneumatic clamp (Fig. 3a). Fig. 3b shows an example setup for a single heating characterization test of the PCB-embedded half-bridge module.

To identify the measurement repeatability for a particular set of test conditions, a method similar to that described in section 3.4 of [13] was applied. For each set of test conditions, five heating curves were measured with thermal grease between the case and the copper standoff and five heating curves were

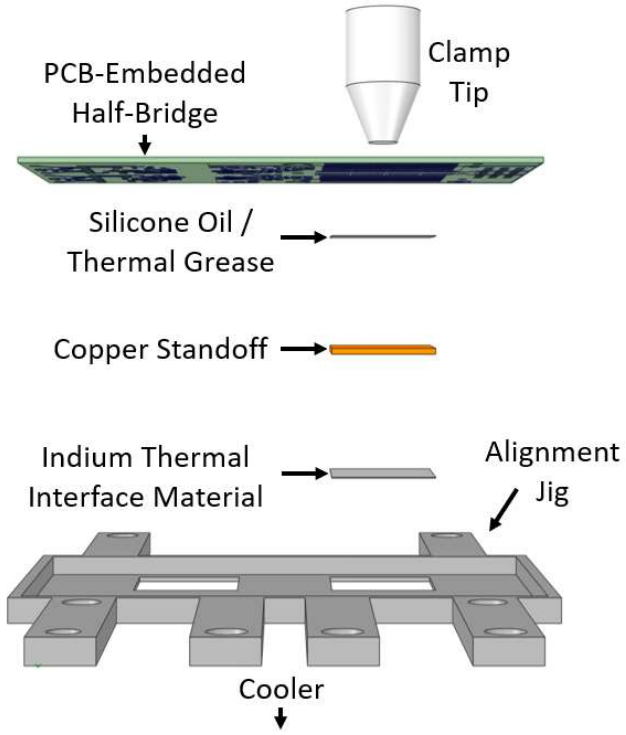

(a)

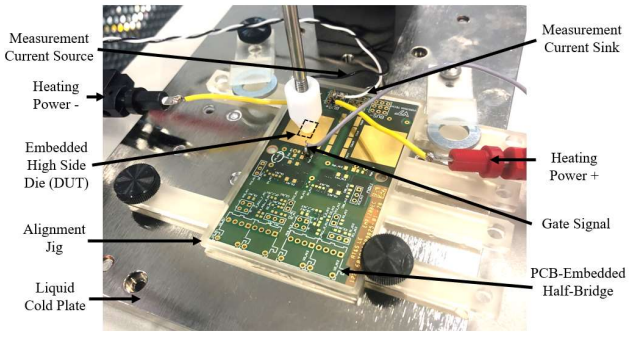

(b)

Fig. 3. (a) An exploded side view of the heating characterization test setup and (b) an example of the PCB-embedded half-bridge module mounted to the liquid cooled test fixture for a heating characterization test.

measured with silicone oil between the case and the copper standoff. After the two sets of five heating curves were collected, they were evaluated pair-wise using the TDIM method described above to obtain 25 $R_{TH,JC}$ values. The average, standard deviation, and maximum deviation for each set of $R_{TH,JC}$ measurements are reported.

The test conditions studied are listed in Table I. These test conditions were chosen because they have the potential to greatly impact the heat flow path. The one exception is the negative gate voltage applied during T_J measurement which was chosen due to concerns about threshold voltages of SiC MOSFETs drifting when high negative biases are applied while current flows through the body diode [19]. The control values in Table I were chosen based on recommendations from Analysis Tech and the JEDEC JESD51-14 standard. The alternative values are used to determine which conditions have an impact on the measured $R_{TH,JC}$.

The accuracy of $R_{TH,JC}$ measurements is more difficult to evaluate. As pointed out in [13], no reliable reference values exist. Measurements using standards which employ TCs are not accurate enough to serve as references. Finite element analysis (FEA) is another option, but it comes with its own challenges such as properly modeling the die attach, accurately meshing complex geometries, and estimating the convection coefficient of the cold plate. Instead, it is proposed that a commercially available package containing the same die as the package under test be subjected to the same set of measurement conditions to provide a reference. Here, a TO-247 package containing the same SiC MOSFET is used to provide that reference [20].

III. Results and Discussion

This section presents the results of the $R_{TH,JC}$ measurements taken in this work and some associated analysis. The first subsection presents the results of a repeatability study used to determine which test conditions in Table I contribute to the deviation of $R_{TH,JC}$ measurements. Subsection B contains statistical analysis performed on the same sets of data to determine which sets have average measured $R_{TH,JC}$s that are significantly different from the control set's average $R_{TH,JC}$. The results of thermal simulations which support some of the conclusions drawn in subsections A and B are provided in subsection C. A method for reducing the deviation in a set of $R_{TH,JC}$ measurements is proposed in subsection D. The final subsection presents the $R_{TH,JC}$ measurements collected under control conditions for a TO-247 package containing the same SiC MOSFET die as the PCB-embedded package. The TO-247 $R_{TH,JC}$ measurements provide a commercially-available reference for the PCB-embedded package's $R_{TH,JC}$ measurements.

A. Repeatability Study

The sets of 25 measured $R_{TH,JC}$s for the PCB-embedded package under seven different sets of test conditions –one test used all control values and the remaining tests used one alternative value each– are provided in Table II - Table VIII. The diagonal borders in the tables indicate heating curve pairs that were deemed too similar –<5% maximum difference– to extract an $R_{TH,JC}$ from their comparison. At first glance, this appears to be a hinderance to the analysis of the data; however, the presence and quantity of failed measurements actually provides an additional metric with which to characterize the sets of $R_{TH,JC}$ measurements. The presence of a failed measurement is undesirable, so test conditions that result in more failed measurements are less ideal. The only two sets without failed measurements are the 2 mm standoff set (Table IV) and the Dow Corning TC-5026 set (Table VII).

TABLE I. Test Conditions Studied

Condition	Control Values	Alternative Values
Pressure (PSI)	10	55
Thermal grease (thermal conductivity)	Dow Corning 340 (0.5 W/mK)	Dow Corning TC-5026 (2.9 W/mK)
Thermal grease thickness (mil)	2	4
Copper standoff thickness (mm)	1	2
Negative gate voltage applied during junction temperature measurement (V)	-5.5	-14
Clamp tip style	Standard	Custom design

TABLE II. Repeated TDIM $R_{TH,JC}$ Measurements - Control

$R_{TH,JC}$ [K/W]		Measurement with Silicone Oil				
		1	2	3	4	5
Measurement with Thermal Grease	1	0.346	0.207			
	2	0.186	0.177	0.186	0.195	0.177
	3	0.186	0.161	0.169	0.186	0.161
	4	0.295	0.189	0.174	0.305	0.174
	5	0.205	0.156	0.156	0.205	0.156

TABLE III. Repeated TDIM $R_{TH,JC}$ Measurements – 4 mil Thermal Grease

$R_{TH,JC}$ [K/W]		Measurement with Silicone Oil				
		1	2	3	4	5
Measurement with Thermal Grease	1	0.238	0.402	0.252	0.34	0.227
	2	0.187	0.464	0.252	0.397	0.207
	3			0.264	0.382	0.25
	4				0.265	0.227
	5					0.25

TABLE IV. Repeated TDIM $R_{TH,JC}$ Measurements – 2 mm Standoff

$R_{TH,JC}$ [K/W]		Measurement with Silicone Oil				
		1	2	3	4	5
Measurement with Thermal Grease	1	0.388	0.34	0.439	0.34	0.457
	2	0.321	0.307	0.336	0.307	0.336
	3	0.445	0.319	0.498	0.319	0.498
	4	0.444	0.292	0.479	0.319	0.497
	5	0.427	0.333	0.46	0.333	0.46

TABLE V. Repeated TDIM RTH,JC Measurements – -14 V Gate Turn-Off

$R_{TH,JC}$ [K/W]		Measurement with Silicone Oil				
		1	2	3	4	5
Measurement with Thermal Grease	1	0.349				
	2	0.348	0.378			
	3	0.404	0.517			
	4	0.244	0.361	0.222		
	5	0.268	0.377	0.244	0.28	

TABLE VI. REPEATED TDIM $R_{TH,JC}$ MEASUREMENTS – CUSTOM CLAMP TIP

$R_{TH,JC}$ [K/W]		Measurement with Silicone Oil				
		1	2	3	4	5
Measurement with Thermal Grease	1	0.252	0.271	0.298	0.298	0.271
	2	0.305	0.28	0.261	0.335	0.305
	3				0.27	0.27
	4	0.226				
	5	0.226	0.174			

TABLE VII. REPEATED TDIM $R_{TH,JC}$ MEASUREMENTS – 55 PSI PRESSURE

$R_{TH,JC}$ [K/W]		Measurement with Silicone Oil				
		1	2	3	4	5
Measurement with Thermal Grease	1	0.237				
	2	0.185	0.15	0.157	0.157	0.216
	3	0.275	0.209	0.209	0.275	0.301
	4	0.194	0.151	0.158	0.186	0.225
	5	0.265	0.201	0.201	0.265	0.291

TABLE VIII. REPEATED TDIM $R_{TH,JC}$ MEASUREMENTS – DOW CORNING TC-5026

$R_{TH,JC}$ [K/W]		Measurement with Silicone Oil				
		1	2	3	4	5
Measurement with Thermal Grease	1	0.146	0.121	0.121	0.146	0.121
	2	0.207	0.151	0.139	0.207	0.139
	3	0.207	0.151	0.139	0.207	0.139
	4	0.146	0.122	0.122	0.146	0.122
	5	0.146	0.121	0.121	0.146	0.127

The averages, standard deviations, and maximum deviations for each set of $R_{TH,JC}$ measurements are listed in Table IX. There is also a box and whisker plot of each set of $R_{TH,JC}$ measurements in Fig. 4. From Table IX and Fig. 4, the Dow Corning TO-5026 has the lowest standard and maximum deviations. Since the Dow Corning TO-5026 has a higher thermal conductivity than Dow Corning 340, it tends to separate more from the silicone oil curve, creating a clearer divergence point. A clearer divergence point leaves less room for error to impact the $R_{TH,JC}$ determination.

B. Statistical Significance of the Varied Test Conditions

To determine which test conditions result in measured $R_{TH,JC}$ averages that are significantly different from those in the control set, the data was analyzed in the statistical analysis software JMP. The treatment in this case was the different sets of test conditions and the response was the measured $R_{TH,JC}$s. The goal of this analysis was to use Tukey's honestly significant difference (HSD) method to determine which sets of test

TABLE IX. AVERAGES, STANDARD DEVIATIONS, AND MAXIMUM DEVIATIONS

EXPERIMENT	AVERAGE (K/W)	STANDARD DEVIATION (K/W)	MAXIMUM DEVIATION (K/W)
CONTROL	0.198	0.0498	0.148
4 MIL THERMAL GREASE	0.288	0.0793	0.176
2 MM STANDOFF	0.388	0.0713	0.110
-14 V GATE TURN-OFF	0.333	0.0813	0.184
CUSTOM CLAMP TIP	0.269	0.0382	0.0955
55 PSI PRESSURE	0.215	0.0473	0.0863
DOW CORNING TO-5026	0.146	0.0285	0.0606

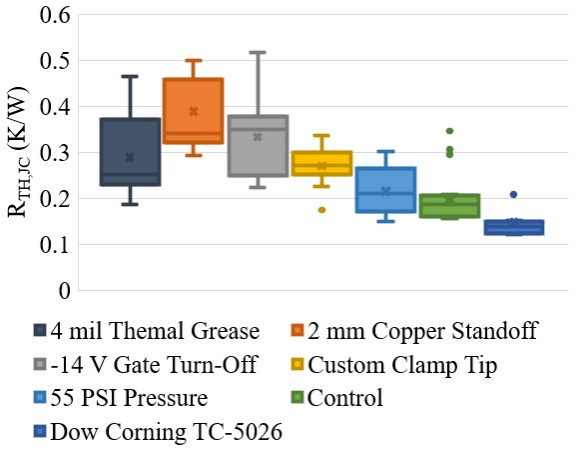

Fig. 4. Box and whisker plots of the PCB-embedded half-bridge's measured $R_{TH,JC}$s under the different sets of conditions from Table I.

conditions, if any, result in measured $R_{TH,JC}$ averages that are significantly different from that of the control set. Before Tukey's HSD method can be applied, however, an analysis of variance (ANOVA) analysis was required to determine if there is a treatment effect at all. For this ANOVA analysis, a significance level (α) of 0.05 was chosen. This means the confidence interval on the result of the analysis is 95%. Equations (2) and (3) list the null hypothesis (H_0) and alternative hypothesis (H_a), respectively. Here μ_i is the mean response under treatment i. The output of this ANOVA analysis is seen in Table X. Since the p-value is less than 0.05 –in fact it is <.0001– H_0 is rejected. There is sufficient statistical evidence to conclude that the different sets of test conditions have some effect on the measured $R_{TH,JC}$.

$$H_0: \mu_1 = \cdots = \mu_7 \quad (2)$$

$$H_a: \mu_i \neq \mu_j \; for \; some \; i \neq j \quad (3)$$

With the ANOVA analysis complete and the conclusion that there is a treatment effect, Tukey's HSD was performed. One way to analyze the results of Tukey's HSD is what's called an ordered letters report. The ordered letters report created from the results of the Tukey's HSD performed here is seen in Table XI. As with any ordered letter report, levels that are not connected by the same letter are significantly different. In this case, the 2 mm copper standoff, the -14 V gate turn-off, the 4 mil thermal grease, and the custom clamp tip datasets were found to be significantly different than the control group dataset. The 55 PSI pressure and the Dow Corning TC-5026 datasets were found to not be significantly different than the control group dataset.

C. Thermal Simulations

Thermal simulations using Ansys Workbench steady state thermal FEA were performed to help support some of the conclusions drawn in the past two subsections. Specifically these simulations were used to help explain why the set of $R_{TH,JC}$

TABLE X. ANOVA OUTPUT

Source	DF	Sum of Squares	Mean Square	F Ratio
Model	6	0.9340446	0.155674	44.5517
Error	129	0.4507559	0.003494	**Prob > F**
C. Total	135	1.3848005		<.0001

TABLE XI. TUKEY'S HSD ORDERED LETTERS REPORT

Level						Least Sq Mean
2 mm Copper Standoff	A					0.38776000
-14 V Gate Turn-Off	A	B				0.33266667
4 mil Thermal Grease		B				0.28775000
Custom Clamp Tip		B	C			0.26946667
55 PSI Pressure			C	D		0.21466667
Control				D	E	0.19781818
Dow Corning TC-5026					E	0.14640000

measurements taken with Dow Corning TO-5026 as the thermal grease had lower standard and maximum deviations than the $R_{TH,JC}$ measurements taken under control conditions, but was not deemed significantly different. To do so, three separate simulations were performed under similar conditions.

In each simulation, loss was applied to the junction of one of the SiC MOSFET die in the PCB-embedded package in a 25 ºC environment with a 1000 W/m^{2}K convection coefficient –to replicate a cold plate [21]– applied to the surface of a 2 mil thick TIM. In simulations one through three, the TIM and loss applied to the junction of the SiC MOSFET were silicone oil and 15 W, Dow Corning 340 and 19.7 W, and Dow Corning TC-5026 and 21.1 W, respectively. The resultant cross sectional temperature distributions and drain-side case heat flux distributions are seen in Fig. 5 and Fig. 6, respectively. Different loss was applied in each simulation to replicate measurement conditions where the maximum T_J was kept constant in each heating curve measurement.

The temperature distributions and the heat flux distributions tell a similar story. The differences between the silicone oil and the Dower Corning 340 distributions are more dramatic than the differences between the Dow Corning 340 and the Dow Corning TC-5026 distributions. The small change seen in the two thermal grease distributions is sufficient to widen the steady state thermal impedance gap between the silicone oil and thermal grease heating curves. The wider gap leads to a more clear divergence point and less variability in the resultant $R_{TH,JC}$ measurement. However, the differences seen in the Dow Corning 340 and the Dow Corning TC-5026 distributions are

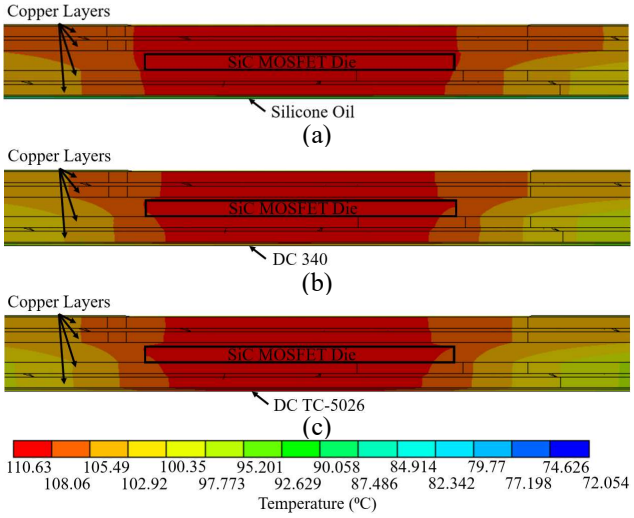

Fig. 5. Simulated temperature distributions around one die in the PCB-embedded 1.2 kV SiC half-bridge package in a 25 ºC environment with 1000 W/m^{2}K convection coefficient applied to the surface of 2 mil thick (a) silicone oil, (b) Dow Corning 340, and (c) Dow Corning TC-5026 with 15 W, 19.7 W, and 21.1 W applied to the die junction, respectively.

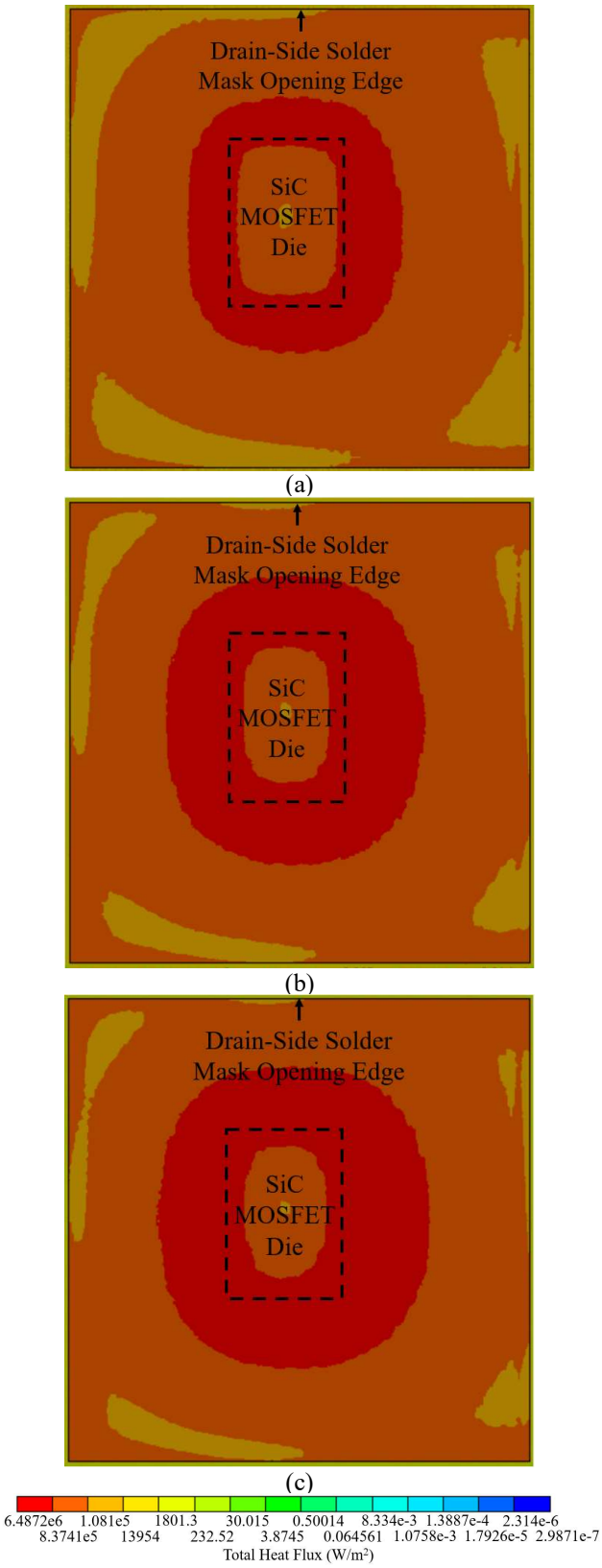

Fig. 6. Simulated heat flux distributions around one die in the PCB-embedded 1.2 kV SiC half-bridge package in a 25 ºC environment with 1000 W/m^{2}K convection coefficient applied to the surface of 2 mil thick (a) silicone oil, (b) Dow Corning 340, and (c) Dow Corning TC-5026 with 15 W, 19.7 W, and 21.1 W applied to the die junction, respectively.

insufficient to lead to a statistically significant difference in their average measured $R_{TH,JC}$s.

D. Reducing Deviation Through Visual Analysis

While collecting the repeatability study measurements, an interesting correlation was identified. The heating curves associated with the measurements highlighted in red in Table XII –which contains identical $R_{TH,JC}$ values as Table II– have poor overlap like those seen in Fig. 1a. Those measurements also happen to be the highest and lowest values in the dataset. This correlation between heating curves with poor overlap and resultant $R_{TH,JC}$ measurements that deviate significantly from the mean is consistent across all seven sets of measurements performed in the repeatability study.

If those values are removed from the set of control measurements seen in Table XII, the standard deviation drops from 0.0498 K/W to 0.0115 K/W and the maximum deviation drops from 0.148 K/W to 0.0167 K/W. With the $R_{TH,JC}$ measurements resulting from heating curves that display poor overlap excluded, the control group has a maximum deviation of 8.76 %. While the standard and maximum deviations change dramatically, the average only changes from 0.198 K/W to 0.191 K/W.

E. TO-247 Reference Measurements

As explained in section II, the $R_{TH,JC}$ of a TO-247 package containing the same SiC MOSFET as the PCB-embedded package was measured to provide a commercially available reference for the PCB-embedded package measurements. The

TABLE XII. REPEATED TDIM $R_{TH,JC}$ MEASUREMENTS - CONTROL

$R_{TH,JC}$ [K/W]		Measurement with Silicone Oil				
		1	2	3	4	5
Measurement with Thermal Grease	1	0.346	0.207			
	2	0.186	0.177	0.186	0.195	0.177
	3	0.186	0.161	0.169	0.186	0.161
	4	0.295	0.189	0.174	0.305	0.174
	5	0.205	0.156	0.156	0.205	0.156

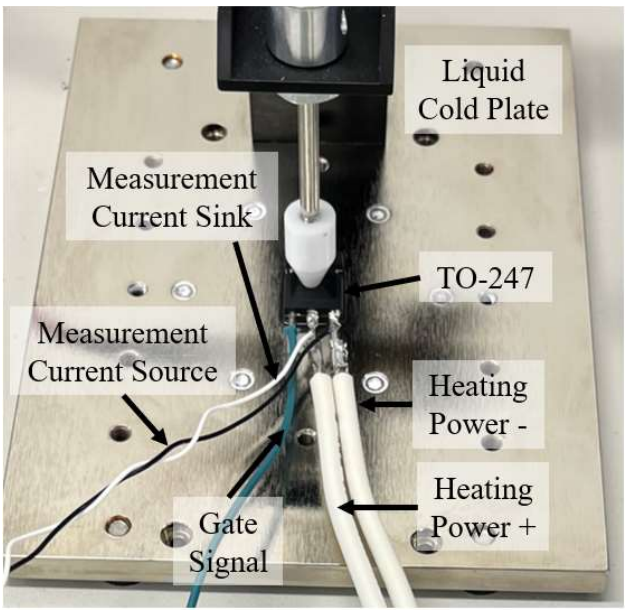

Fig. 7. An example of a TO-247 package mounted to the liquid cooled test fixture for a heating characterization test.

TABLE XIII. REPEATED TDIM $R_{TH,JC}$ MEASUREMENTS – TO-247 CONTROL

$R_{TH,JC}$ [K/W]		Measurement with Silicone Oil				
		1	2	3	4	5
Measurement with Thermal Grease	1	0.249	0.23	0.263	0.293	0.212
	2	0.242	0.229	0.256	0.293	0.211
	3	0.242	0.23	0.256	0.293	0.211
	4	0.26	0.222	0.371	0.39	0.26
	5	0.252	0.245	0.331	0.348	0.239

experimental setup used to perform heating characterization tests on a TO-247 package is seen in Fig. 7. The TO-247 package was subjected to the same set of test conditions as the PCB-embedded package was during the control tests. The results from those measurements are seen in Table XIII. The average, standard deviation, and maximum deviation of these measurements are 0.265 K/W, 0.0479 K/W, and 0.125 K/W, respectively. The standard deviation is similar to that found for measurements of the PCB-embedded package's $R_{TH,JC}$ under control test conditions.

IV. CONCLUSIONS

The test conditions used when measuring the $R_{TH,JC}$ of a package can have a significant impact on the measurement accuracy and repeatability. When using the TDIM, the two selected TIMs should allow for a clear divergence point while maintaining the same heat flow path. It is important to apply TIMs consistently; viscous TIMs should be screen printed and less viscous TIMs should be applied using a pipette. Here it was also found that measurement sets resulting from alternative copper standoff thickness, negative gate bias, thermal grease thickness, and clamp tip style have statistically significant differences in $R_{TH,JC}$ measurement mean compared to the control set. Thermal grease thermal conductivity was found to impact the standard and maximum deviations of $R_{TH,JC}$ measurements. A method for reducing the standard and maximum deviations through visual analysis of the compared heating curves was introduced. Finally, the $R_{TH,JC}$ of a TO-247 package was measured to provide a commercially-available reference for the PCB-embedded package. The work done here to explore the impact of test conditions on $R_{TH,JC}$ measurements is by no means exhaustive. It is still highly recommended that test conditions be reported along with $R_{TH,JC}$ measurement results.

ACKNOWLEDGEMENT

The authors appreciate AT&S for supplying the PCB-embedded half-bridge packages and Hannes Stahr, Mike Morianz, Thomas Koeck, and Gerald Weis for supporting their design.

REFERENCES

[1] V. B. Dutta, "Junction-to-case thermal resistance-still a myth?," in *Fourth Annual IEEE Semiconductor Thermal and Temperature Measurement Symposium*, Feb. 1988, pp. 8–11. doi: 10.1109/SEMTHE.1988.10590.

[2] A. Bar-Cohen, T. Elperin, and R. Eliasi, "theta /sub jc/ characterization of chip packages-justification, limitations, and future," *IEEE Transactions on Components, Hybrids, and Manufacturing Technology*, vol. 12, no. 4, pp. 724–731, Dec. 1989, doi: 10.1109/33.49039.

[3] J. E. Galloway, S. Bhopte, and C. Nelson, "Characterizing junction-to-case thermal resistance and its impact on end-use applications," in *13th InterSociety Conference on Thermal and Thermomechanical Phenomena in Electronic Systems*, May 2012, pp. 1342–1347. doi: 10.1109/ITHERM.2012.6231576.

[4] C. Yue, J. Lu, X. Zhang, and Y.-S. Ho, "Effects of package type, die size, material and interconnection on the junction-to-case thermal resistance of power MOSFET packages," in *2011 12th International Conference on Electronic Packaging Technology and High Density Packaging*, Aug. 2011, pp. 1–6. doi: 10.1109/ICEPT.2011.6066900.

[5] S. Lu, Z. Zhang, C. Buttay, K. D. T. Ngo, and G.-Q. Lu, "Improved Measurement Accuracy for Junction-to-Case Thermal Resistance of GaN HEMT Packages by Gate-to-Gate Electrical Resistance and Stacking Thermal Interface Materials," *IEEE Transactions on Power Electronics*, vol. 37, no. 6, pp. 6285–6289, Jun. 2022, doi: 10.1109/TPEL.2022.3142273.

[6] A. Griffo, J. Wang, K. Colombage, and T. Kamel, "Real-Time Measurement of Temperature Sensitive Electrical Parameters in SiC Power MOSFETs," *IEEE Transactions on Industrial Electronics*, vol. 65, no. 3, pp. 2663–2671, Mar. 2018, doi: 10.1109/TIE.2017.2739687.

[7] J. O. Gonzalez, O. Alatise, J. Hu, L. Ran, and P. A. Mawby, "An Investigation of Temperature-Sensitive Electrical Parameters for SiC Power MOSFETs," *IEEE Transactions on Power Electronics*, vol. 32, no. 10, pp. 7954–7966, Oct. 2017, doi: 10.1109/TPEL.2016.2631447.

[8] H. Yu, X. Jiang, J. Chen, Z. J. Shen, and J. Wang, "Comparative Study of Temperature Sensitive Electrical Parameters for Junction Temperature Monitoring in SiC MOSFET and Si IGBT," in *2020 IEEE 9th International Power Electronics and Motion Control Conference (IPEMC2020-ECCE Asia)*, Nov. 2020, pp. 905–909. doi: 10.1109/IPEMC-ECCEAsia48364.2020.9367830.

[9] J. Chen, E. Deng, Y. Zhang, and Y. Huang, "Junction-to-Case Thermal Resistance Measurement and Analysis of Press-Pack IGBTs Under Double-Side Cooling Condition," *IEEE Transactions on Power Electronics*, vol. 37, no. 7, pp. 8543–8553, Jul. 2022, doi: 10.1109/TPEL.2022.3151411.

[10] *Semiconductor Devices – Discrete Devices – Part 15: Isolated Power Semiconductor Devices*. IEC 60747-15:2010, 2012.

[11] R. L. Kozarek, "Effect of case temperature measurement errors on the junction-to-case thermal resistance of a ceramic PGA," in *1991 Proceedings, Seventh IEEE Semiconductor Thermal Measurement and Management Symposium*, Feb. 1991, pp. 44–51. doi: 10.1109/STHERM.1991.152910.

[12] *Transient Dual Interface Test Method for the Measurement of the Thermal Resistance Junction-to-Case of Semiconductor Devices with Heat Flow Through a Single Path*. JESD51-14, 2010.

[13] D. Schweitzer, H. Pape, L. Chen, R. Kutscherauer, and M. Walder, "Transient dual interface measurement — A new JEDEC standard for the measurement of the junction-to-case thermal resistance," in *2011 27th Annual IEEE Semiconductor Thermal Measurement and Management Symposium*, Mar. 2011, pp. 222–229. doi: 10.1109/STHERM.2011.5767204.

[14] E. Deng, Z. Zhao, P. Zhang, J. Li, and Y. Huang, "Study on the Method to Measure the Junction-to-Case Thermal Resistance of Press-Pack IGBTs," *IEEE Transactions on Power Electronics*, vol. 33, no. 5, pp. 4352–4361, May 2018, doi: 10.1109/TPEL.2017.2718245.

[15] E. Deng, W. Chen, P. Heimler, and J. Lutz, "Temperature Influence on the Accuracy of the Transient Dual Interface Method for the Junction-to-Case Thermal Resistance Measurement," *IEEE Transactions on Power Electronics*, vol. 36, no. 7, pp. 7451–7460, Jul. 2021, doi: 10.1109/TPEL.2020.3042495.

[16] T. Yin *et al.*, "Thermal resistance measurement of packaged SiC MOSFETs by transient dual interface method," in *2017 IEEE 24th International Symposium on the Physical and Failure Analysis of Integrated Circuits (IPFA)*, Jul. 2017, pp. 1–4. doi: 10.1109/IPFA.2017.8060196.

[17] J. Knoll, G. Son, C. DiMarino, Q. Li, H. Stahr, and M. Morianz, "Design and Analysis of a PCB-Embedded 1.2 kV SiC Half-Bridge Module," in *2021 IEEE Energy Conversion Congress and Exposition (ECCE)*, Oct. 2021, pp. 5240–5246. doi: 10.1109/ECCE47101.2021.9596034.

[18] ON Semiconductor, "MOSFET - n-channel, silicon carbide 1200 V, 20 mΩ." NVC020N120SC1 datasheet, Jun. 2020.

[19] O. Aviño Salvado, H. Morel, C. Buttay, D. Labrousse, and S. Lefebvre, "Threshold Voltage Instability in SiC MOSFETs as a Consequence of Current Conduction in Their Body Diode," *Microelectronics Reliability*, vol. 88–90, pp. 636–640, 2018, doi: 10.1016/j.microrel.2018.06.033.

[20] ON Semiconductor, "MOSFET - SiC power, single n-channel." NTHL020N120SC1 datasheet, Apr. 2021.

[21] P. G. Kosky, R. T. Balmer, W. Keat, and G. Wise, Eds., *Exploring engineering: an introduction to engineering and design*, Third edition. Burlington, MA: Elsevier/AP, 2013.